

X-Band MEMS Capacitive Shunt Switches with Metal-Insulator-Metal Contacts for Improved Isolation

T. Ketterl⁽¹⁾ and T. Weller⁽²⁾

(1) Center for Ocean Technology, University of South Florida, St. Petersburg, FL 33701

(2) Department of Electrical Engineering, University of South Florida, Tampa, FL 33620

tketterl@marine.usf.edu

Abstract

This paper introduces MEMS electro-statically actuated switches that utilize a fixed metal-insulator-metal (MIM) structure for capacitive coupling with a movable shunt bridge to improve the isolation in the off-state. These switches, with single and dual beams, were designed for operation in the X-band frequency range using fixed inductive line section. The advantage of this design is that the isolation, which is directly related to the quality of the capacitive coupling in the actuated state, is not dependent on the planarity of the movable beam structure. Isolations greater than 45 dB and 35 dB at 10 GHz were measured for the double and single beam switches, respectively. From 8 to 12 GHz, an insertion loss of less than 0.3 dB was measured in the on-state for both switch designs. Switching speeds of 40 and 70 μ s for the rise and fall times, respectively, of the single beam switch were also measured.

1. Introduction

In recent years, the utilization of MEMS technology in radio and microwave frequency (RF/Microwave) and wireless engineering applications has seen rapid growth and development. MEMS fabricated switches are an example of devices in this innovative field and have already shown superior electrical performances (isolation, insertion loss, DC power consumption, and intermodulation products) to solid state p-i-n and field effect transistor (FET) switches at high frequencies [1]. Due to these qualities, as well as their small size and their manufacturability using well characterized semiconductor processing techniques, RF MEMS switches have the potential to be a viable replacement to their solid state switch counterparts. Examples of

RF circuit components, where the tuning capability of RF MEMS switches have been shown to play an intrinsic role, include tunable resonators [2], capacitors [3], inductors [4], transmission lines [5] and antennas [6].

Since RF MEMS switches generally consist of a movable membrane that makes or breaks an electrical contact to provide isolation or insertion loss, it is important to achieve near perfect planar actuation structures during the fabrication procedure. Non-uniformities in the membranes can occur when residual stresses, that result during the fabrication process, cause the structures to bend after the release step. This can significantly degrade the switch performance in the actuated state, whether the coupling mechanism is DC contact or capacitive in nature. In the first case, contact resistance is increased due to the resulting smaller contact area. In the latter case, the overall coupling capacitance is reduced.

In this paper, a fixed metal pad was placed on top of the dielectric during the fabrication process to eliminate the dependence on the quality of the membrane shape for MEMS switches with capacitive coupling. This configuration is equivalent to having a fixed metal-insulator-metal (MIM) capacitor in the lower electrode as shown in Figure 1. With actuation, capacitive coupling level is now independent of the resulting shape of the MEMS beam; i.e. since there is now metal-to-metal contact with a MIM capacitor that has a fixed capacitance value, the effects of residual stress will not contribute to the effective capacitance value in the down state. The online draw-back to this change is that the isolation is now dependent on the quality of the down state contact resistance between the beam and MIM metal.

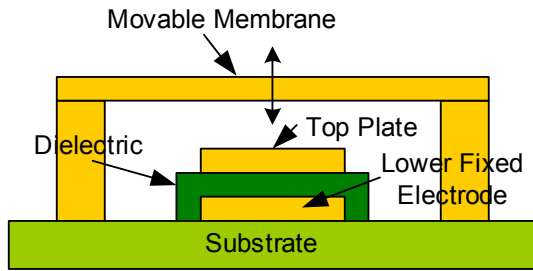


Figure 1. Capacitive RF MEMS switch with added fixed metal plate on top of dielectric

The MEMS switches in this investigation, which were designed with the MIM structure, utilize coplanar waveguide topology and electro-statically actuated shunt MEMS beam structures. These beams provide isolation in the actuated state (off-state) by coupling the input signal to the ground planes. In the un-actuated state (on-state) with the beams suspended over the center conductor, signal transmission with low insertion loss is achieved. The operational frequency range of the switches was 8 to 12 GHz. By including thin inductive line sections that connect the base of the beam structures to the ground planes, the resonant frequency, which occurs due to the interaction between the inductive lines and the MIM capacitance in the actuated state, could be tuned down to 10 GHz. Switches with single and dual beams, as shown in Figure 2, were fabricated and tested. Isolations greater than 45 dB and 35 dB at 10 GHz were measured for the double and single beam shunt switches, respectively. From 8 to 12 GHz, an insertion loss of less than 0.3 dB was measured in the on-state for both switch designs. Switching speeds of 40 and 70 μ s for the rise and fall times, respectively, of the single beam switch were also measured.

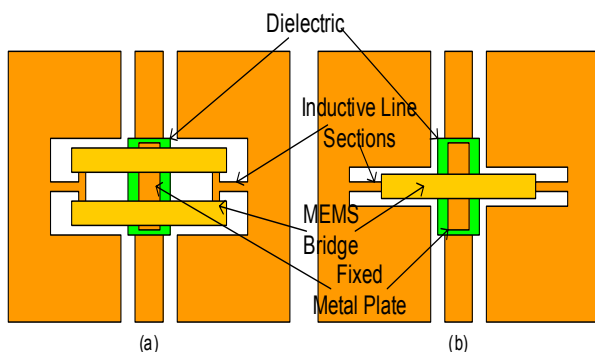


Figure 2. Layout of double beam (a) and single beam (b) MEMS shunt switches.

2. Switch Design and Fabrication

The switches were designed using high resistivity ($\rho > 3000 \Omega$) silicon as the substrate material with a thickness of about 400 μ m. The transmission line components of the MEMS switch were designed as a CPW transmission line with grounded substrate having a 50 Ω characteristic impedance, which corresponds to a center conductor width (w) of 100 μ m and a ground-to-center spacing (s) of 50 μ m. In this design, the top plate had a width of 100 μ m and a length of 200 μ m. The fixed-fixed bridges of the shunt switches were 415 μ m long and 60 μ m wide. The inductive line section in the shunt switch designs were 15 x 100 μ m in size.

The fabrication of the switches is illustrated in Figure 3 and begins with (1) a 3,000 \AA thick thermally evaporated gold layer, with a thin chromium adhesion layer underneath, using a metal lift-off process. A 2800 \AA thick PECVD dielectric layer (silicon nitride) is then deposited over the center conductor and patterned and etched using a RIE tool. This was followed by the metal top plate which consists of a 1000 \AA thick thermally evaporated Cr/Au layer. (2) PMMA was chosen as the sacrificial material and was spun on top of the sample to obtain a thickness of 1.5 μ m. After the PMMA was patterned with the remainder of the CPW transmission lines structures, using oxygen plasma etching and photoresist as the masking layer, a thin (400 \AA) Au/Cr seed layer was thermally deposited on top of the sample followed by an application of spun-on photo resist; this was required for the subsequent electroplating process of the MEMS cantilevers. (3) After the cantilever geometry was patterned and the resist developed to provide a plating mask for the cantilevers, electroplating of the seed layer was performed to obtain 1 μ m thick beams. After the plating mask was removed, the cantilevers were protected with photoresist, the seed layer was removed using Cr and Au enchants, and the sacrificial layer was removed using MicroChem 1165 photoresist stripper and rinsed in a series of methanol baths. (4) The final release process involved the use of a critical point dryer (CPD) that entails heating the samples above the critical point of the liquid it is immersed in. This process is required to eliminate stiction of the MEMS cantilevers that can be caused by evaporation of the methanol. Optical images of the fabricated switches are shown in Figure 4.

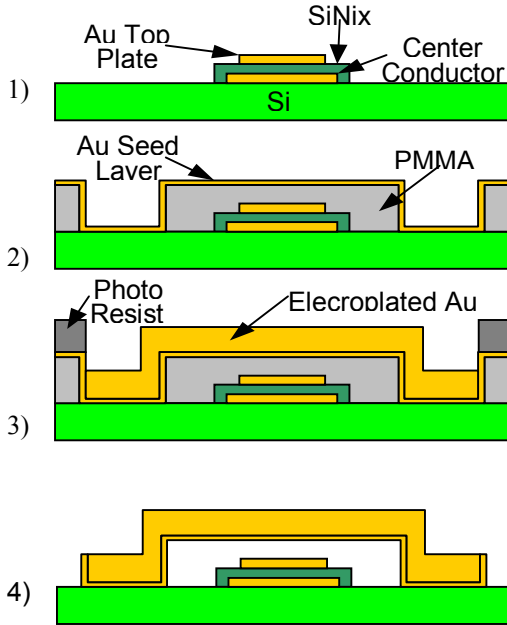


Figure 3. Processing steps of the RF MEMS switches with capacitive top plate.

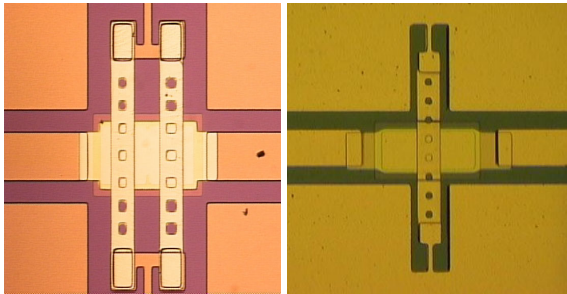


Figure 4. Optical images of fabricated double (left) and single (right) bridge MEMS switches.

3. Measured Results

Measurements were performed on a Wiltron 360 VNA with a Karl Suss probe station and 150 μm pitch G-S-G (ground-signal-ground) probes. S-parameter measurements were collected using Wincal software and the data was imported into Agilent's ADS [7] microwave circuit simulator. DC biasing was accomplished through the RF probes using bias tees to isolate the DC from the RF signals.

A capacitive shunt switch with dual beam design was measured and a comparison between these results and simulated data are shown in Figure 5 and 6. Agilent ADS Momentum was used to simulate the RF performance. At 10 GHz, the isolation was greater than 45 dB with an insertion loss of less about 0.15 dB

at the same frequency. Actuation of the MEMS bridge occurred at about 35 V.

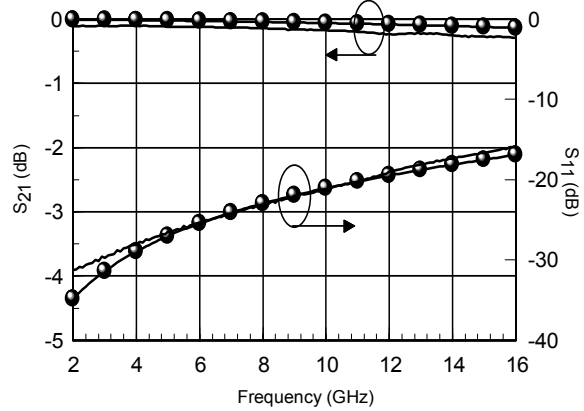


Figure 5. Comparison between measured and simulated S_{11} and S_{21} data of the shunt capacitive MEMS switch with double beams in the up state. Simulated data is shown with double markers and measured data with straight lines.

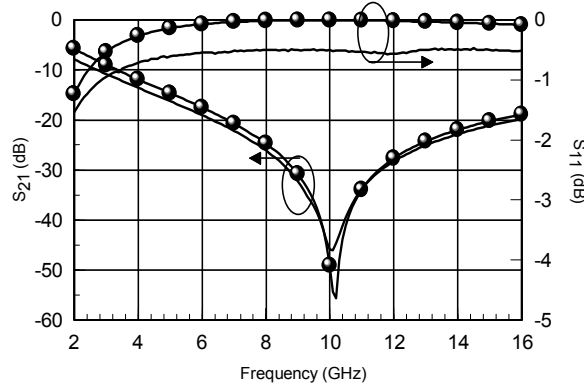


Figure 6. Comparison between measured and simulated S_{11} and S_{21} data of the shunt capacitive MEMS switch with double beams in the down state. Simulated data is shown with markers and measured data with straight lines.

Figure 7 and 8 show the frequency response of the switch with straight inductive line. Insertion losses of less than 0.3 dB were measured with isolation greater than 35 dB at the resonant frequency. For the single beam, 25 V of bias voltage was needed to actuate the device. A lower actuation voltage for the single beam switch, when compared to that of the double beam device, was achieved since the beam metal of the single beam design was about 1 μm , compared to 1.3 μm for the double beam design.

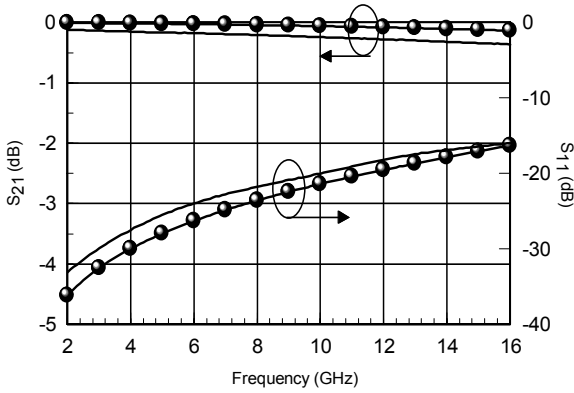


Figure 7. Comparison between measured and simulated S_{11} and S_{21} data of the shunt capacitive MEMS switch with single beam in the up state. Simulated data is shown with markers and measured data with straight lines.

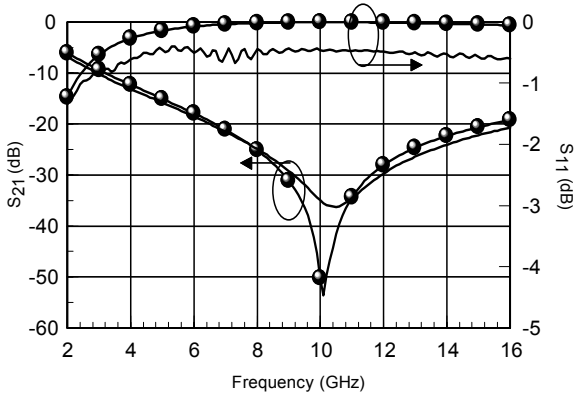


Figure 8. Comparison between measured and simulated S_{11} and S_{21} data of the shunt capacitive MEMS switch with single beam in the down state. Simulated data is shown with markers and measured data with straight lines.

From the measured results, it can be observed that the double beam design provides greater isolation at resonance. This increase in isolation is due to the larger contact area of the double beam structure in the actuated state, which lowers the contact resistance between the movable plate and the MIM top plate.

4. Switching Speed Measurements

Switching speed measurements were performed using the setup shown in the block diagram of Figure 9. To test the switching performance of the fabricated MEMS devices, a 10 GHz signal is injected into the input port of the switches. An arbitrary waveform generator, which is amplified to provide the required voltage to actuate the switch, was used to provide the

modulating signal. A 35 V square wave with 50% duty cycle was used to drive the switch. The modulated 10 GHz output of the switch was then measured using a diode detector. Both the detected modulation waveform and the driving waveform are compared using an oscilloscope.

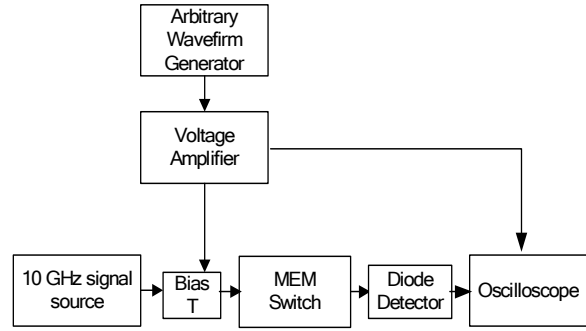


Figure 9. Block diagram of switching speed test setup.

Figure 10 and 11 show screen shots of the fastest rise and fall times of the double beam shunt switch, respectively. The quickest actuation speed was seen to be about 900 μ s with a slightly faster release time of about 500 μ s.

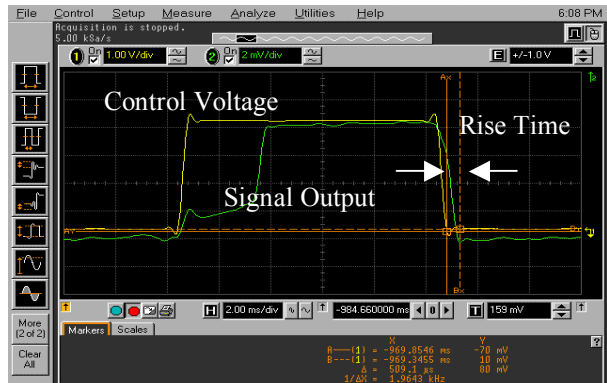


Figure 10. Rise time of double beam shunt switch.

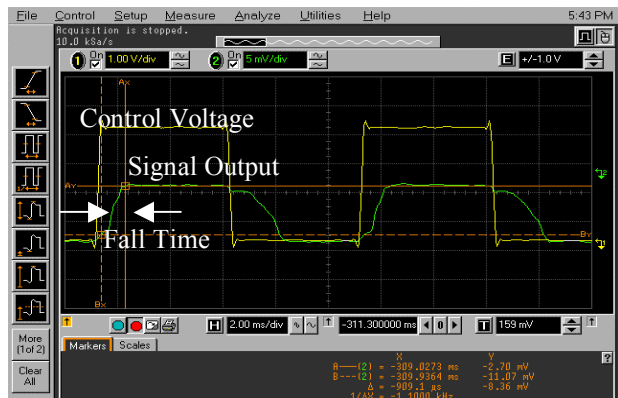


Figure 11. Fall time of double beam shunt switch.

The rise and fall times of the single beam switch decreased significantly to about 80 and 40 μ s, respectively. The fall time of the single beam shunt switch is shown in Figure 12 and the rise time in Figure 13.

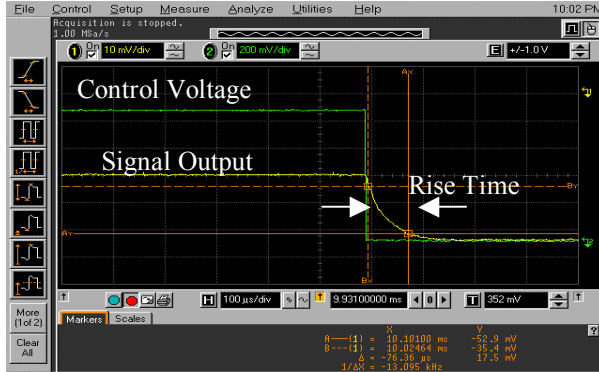


Figure 12. Rise time of single beam shunt switch.

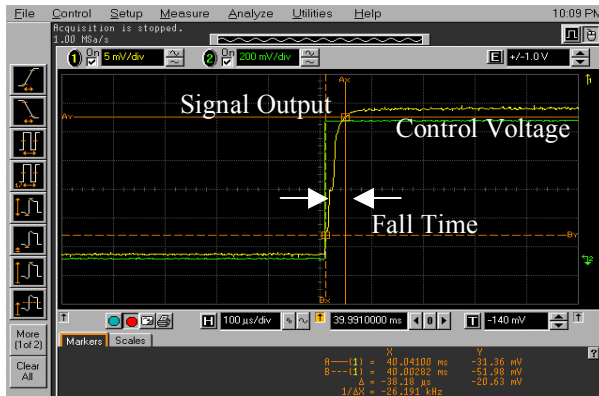


Figure 13. Fall time of single beam shunt switch.

It is believed that the relatively slow switching times of the dual switch design were caused by the separate beam components of the dual beam structure not being able to actuate and release simultaneously, which could be due to a slight discrepancy in beam dimensions caused by a non-uniform fabrication processes.

5. Conclusion

It has been shown that by adding a fixed metal plate on top of a dielectric layer in a conventional RF MEMS shunt switch design, the quality of isolation in the off-state, due to the RF coupling capacitance, can be made independent of the actuation structure shape. Therefore, it is not critical with this design to obtain perfect planar structures during the fabrication process. The measured switches, with single and dual beam designs, showed insertion losses in the on-state

of < 0.3 dB at X-band and isolations of 35 and 40 dB at resonance, respectively. In both cases, the isolation was >25 dB across the X-band frequency range. Switching speeds in the 100's of microseconds and 40 to 80 μ s for the dual and single beam switches, respectively, were also measured. It can therefore be concluded that the shunt switch with the double beam design will provide higher isolation than the single beam switch due to the double beam switch's lower contact resistance in the down state. This characteristic would make the double beam design more suitable for applications where very high isolation at the design frequency is required. However if faster switching speed is more important, the single beam design will provide better rise and fall times.

6. Acknowledgements

This work was supported by the U.S. Army Space and Missile Defense Command, grant number DASG-00-0089. "Distribution A. Approved for Public Release; distribution unlimited"

7. References

- [1] P.D. Grant and M.W. Denhoff, "A comparison between RF MEMS switches and semiconductor switches," *International Conference on MEMS, NANO, and Smart Systems*, pp. 515-521, August 2004.
- [2] T. Ketterl, et. al, "A micromachined tunable CPW resonator," *IEEE MTT-S International Microwave Symposium Digest*, vol. 1, pp. 345-348, May 2001.
- [3] H.D. Wu, "MEMS designed for tunable capacitors," *IEEE MTT-S International Microwave Symposium Digest*, vol. 1, pp. 127-129, June 1998.
- [4] I. Zine-El-Abidine, et. al, "A Tunable RF MEMS Inductor," *International Conference on MEMS, NANO, and Smart Systems*, pp. 636-638, August 2004.
- [5] J.Y. Lee, et. al, "RF MEMS devices," *International Conference on MEMS, NANO, and Smart Systems*, pp. 103-107, July 2003.
- [6] P. Panaia, et. al, "MEMS-Based Reconfigurable Antennas," *IEEE International Symposium on Industrial Electronics*, vol. 1, pp. 175-179, May 2004.
- [7] Advance Design Systems, version 2004A, Agilent Technologies, Palo Alto, CA 94304.